European Radiology (2019) 29:259–269
https://doi.org/10.1007/s00330-018-5592-y

CARDIAC

Optimal pre-TAVR annulus sizing in patients with bicuspid aortic valve: area-derived perimeter by CT is the best-correlated measure with intraoperative sizing

Yuan Wang[1] · Moyang Wang[1] · Guanyuan Song[1] · Wei Wang[2] · Bin Lv[3] · Hao Wang[4] · Yongjian Wu[1]

Received: 24 January 2018 / Revised: 28 May 2018 / Accepted: 4 June 2018 / Published online: 20 June 2018

Abstract

Objective To clarify the optimal measurements for patients with bicuspid aortic valve (BAV) preferred for transcatheter aortic valve replacement (TAVR), our study compared intraoperative sizing with five different approaches by transthoracic echocardiography (TTE), three-dimensional transesophageal echocardiography (3DTEE) and computed tomography (CT).

Methods We enrolled 104 BAV patients prescreened for TAVR but who underwent surgery with direct intraoperative annulus sizing. All five approaches [2DTTE, 3DTEE, area-derived perimeter (CTarea), perimeter-derived diameter (CTperi) and mean diameter (CTmean)] were compared with intraoperative sizing, respectively. Agreements on theoretical valve selections by five methods with those by intraoperative sizing were analyzed.

Results CTarea showed the highest correlation (r = 0.932) and the best agreement with intraoperative sizing. Agreement for theoretical surgical and TAVR prosthesis selection was found in 84.6% and 74.0% BAVs by CTarea (κ = 0.791, κ = 0.585). CTperi-based prosthesis selection led to overestimation of 26.9% for surgical valves (κ = 0.589) and 36.5% for TAVR valves (κ = 0.425). Good correlations were observed between CT measurements and intraoperative sizing regardless of the predominant site of aortic valve calcification (r = 0.860-0.953).

Conclusion The CTarea, which demonstrated the optimal approach to annulus sizing and prosthesis choice of BAVs with high eccentricity, should be included into the BAV-specific annulus sizing recommendation. The insufficiency of CTperi lay in overestimation of surgical or TAVR valve selections. Good agreement of 3DTEE sizing proved its superiority in annulus sizing for BAVs unsuitable for CT, but it should be used with caution for patients with a calcified annulus, where partial acoustic shadowing could lead to image inaccuracy.

Key Points

- *The area-derived perimeter by CT is the optimal approach to annulus sizing of BAVs.*
- *The perimeter-derived approach is prone to overestimation of BAVs.*
- *3DTEE showed its superiority in annulus sizing for BAVs unsuitable for CT, but it should be used with caution in patients with a calcified annulus.*

Keywords Aortic valve · Transcatheter aortic valve replacement · Echocardiography · Multidetector computed tomography · Aortic valve stenosis

Electronic supplementary material The online version of this article (https://doi.org/10.1007/s00330-018-5592-y) contains supplementary material, which is available to authorized users.

✉ Yongjian Wu
fuwai52wardw@126.com

[1] Department of Cardiology, Ward 52, Fuwai Hospital, National Center for Cardiovascular Disease, Chinese Academy of Medical Science and Peking Union Medical College, No.167 Beilishi Rd, Beijing 10037, China

[2] Department of Cardiac Surgery, Fuwai Hospital, National Center for Cardiovascular Disease, Beijing, China

[3] Department of Radiology, Fuwai Hospital, National Center for Cardiovascular Disease, Beijing, China

[4] Department of Ultrasound, Fuwai Hospital, National Center for Cardiovascular Disease, Beijing, China

Abbreviations

BAV Bicuspid aortic valve
BSA Body surface area
TAV Tricuspid aortic valve
TAVR Transcatheter aortic valve replacement

Introduction

Transcatheter aortic valve replacement (TAVR) is currently considered an appealing alternative choice to surgery for severe aortic stenosis patients not only with tricuspid aortic valve (TAV) but also with bicuspid aortic valve (BAV) [1, 2]. The lack of direct open-heart view during TAVR makes it harder to obtain accurate annulus sizing. Incorrect valve selection has been proven to be the principle cause of adverse effects such as annulus rupture and paravalvular aortic regurgitation [3]. With dedicated reconstructions of the three-dimensional data, computed tomography (CT) is the preferred imaging modality in both guidelines and expert consensus [4, 5]. However, information related to the optimal assessment and calculation method for BAV annulus diameter by CT is limited. Given that the pronounced oval-shaped annulus of the BAV is prone to reshape and deform after implantation [6, 7], whether the previously mentioned preferred approach is also suitable for BAVs is unknown.

The aim of our study was to compare direct intraoperative annulus sizing with two-dimensional transthoracic echocardiography (2DTTE), three-dimensional transesophageal echocardiography (3DTEE) and CT results according to the mean, perimeter-derived and area-derived diameters to determine the optimal and best-tailored measurements for patients with BAV.

Material and methods

Study population

This is a retrospective single-center study. The cohort involved 126 patients with bicuspid aortic valve suffering from severe aortic stenosis who were screened for TAVR but received surgical aortic valve replacement after evaluation by the multidisciplinary heart team from March 2013 to September 2016. All patients had at least intermediate surgical risk and underwent preoperative 2DTTE, 3DTEE, CT and intraoperative measurement of the aortic annulus with metric sizers.

Exclusion criteria included an annular diameter beyond the prosthesis size available ($n = 4$), inadequate CT images due to atrial fibrillation, arrhythmias or tachycardia ($n = 11$), and an inadequate echocardiographic window ($n = 7$). In total, 104 patients were included in this study. All patients underwent preoperative 2DTTE, 3DTEE, CT and thus intraoperative measurement of the aortic annulus with a metric sizer. Both the CT laboratory technicians and echocardiographers were blinded to the IDs or names of the patients as well as imaging measurements. All the analyses were performed by two investigators. The institutional ethics committee approved this retrospective study. Oral and written consents were obtained from all patients.

Transthoracic echocardiography and transesophageal echocardiography

TTE was performed by highly experienced echocardiographers with a commercially available system (iE33, Philips Medical System with a S5-1 probe). The aortic annulus was measured in the parasternal long-axis three-chamber view during mid-systole (Fig. 1a). Mean transvalvular gradients and left ventricular ejection fraction were recorded in all patients pre- and postoperatively.

TEE imaging was obtained by the same equipment as for TTE, but with an X7-2t probe in patients undergoing general anesthesia intra-procedurally, prior to the sternotomy. A 2D acquisition in a zoom mode of the left ventricular outflow tract from the mid-esophageal position with scanning plans from 115-160° was performed. Additionally, real-time zoomed 3D images containing the whole aortic apparatus were obtained. The 3D data set was evaluated off-line with commercially available software (3DQ, Q-Lab version 7.0, Philips Medical Systems). Two orthogonal planes parallel bisecting the aortic valve in the long axis were manually adjusted. The third plane was transversal to visualize the short-axis view, and the aortic annulus diameter was measured in systole by the area method (Fig. 1b).

Computed tomography

All patients underwent coronary computed tomography angiography (CCTA) on a second-generation dual-source CT scanner (Somatom Definition Flash, Siemens Healthcare). Retrospective ECG gating was used to evaluate the aortic valve morphology and to detect coronary artery disease with high diagnostic accuracy [5, 8, 9]. Acquisition parameters were as follows: 2 × 64 × 0.6-mm detector collimation and 280-ms gantry rotation time. All studies were acquired in a cranio-caudal direction in end-inspiration. Attenuation-based tube current modulation (CareDose 4D, Siemens) was applied per default. For contrast medium enhancement, automated bolus tracking was used in a region of interest within the ascending aorta, with a signal attenuation trigger threshold of 100 Hounsfield units (HU) and a 6-s scan delay. We used a triple-phase contrast medium injection protocol

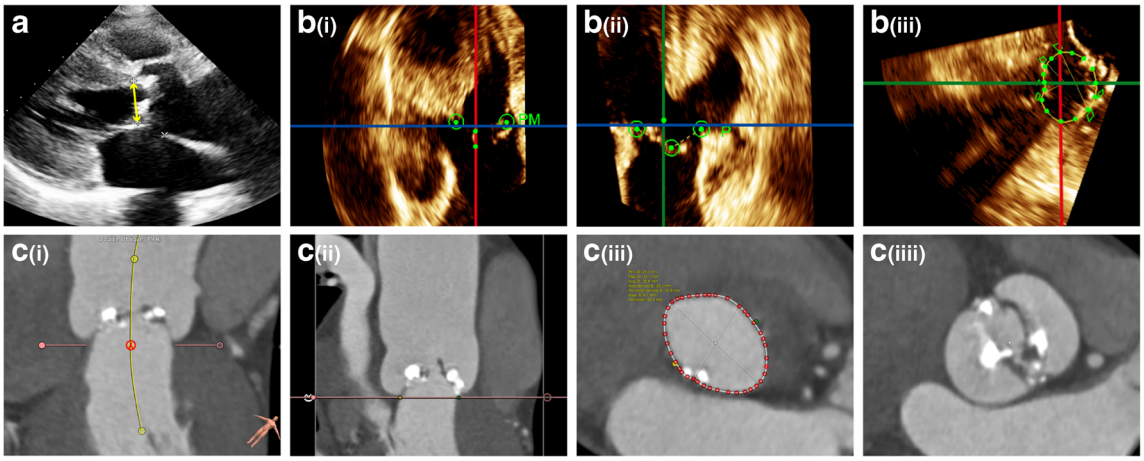

Fig. 1 Measurement of aortic annulus diameter by 2DTTE, 3DTEE and CT. **a** Measurement of aortic annulus diameter by 2DTTE in the parasternal long-axis three-chamber view during mid-systole. **b** Stepwise approach to measurement of aortic annulus diameter by a 3D data set from 3DTEE: The transverse plane (blue plane) of the annulus is identified by alignment of the two orthogonal long-axis views (red and green planes). The hinge point of each individual aortic valve cusp is identified to establish the plane of the annulus. Four plots are placed on orthogonal long-axis images (i and ii) at the level of the annulus. Sixteen plots are adjusted (if needed) and confirmed. Measurement is performed on the short-axis image (iii). **c** Example of measurement of the aortic annulus by CT: (i) A line is generated through the center point of the proximal segment of the ascending aorta, aortic valve, annulus and left ventricular outflow tract. (ii) The basal annular plane is defined as a plane perpendicular to the curved axis that touches the lowest points of the valves. (iii) Tracing of the border of the annulus by placing plots (red dots) at the blood-tissue interface. Data of the perimeter, area, and maximum and minimum diameters are automatically determined by the 3-mensio package after confirmation of all the plots. (iv) The transverse plane is shifted from the annulus to the supravalvular crest, allowing the identification of the bicuspid aortic valve

[10], which consisted of 50 to 60 ml of undiluted contrast agent (iopromide; Ultravist 370 mgI/ml, Bayer Healthcare) followed by a 30-ml 30%: 70% mixture of contrast medium and saline and a 40-ml saline chaser bolus, all injected with flow rates of 4 to 5 ml/s. The mean radiation dose was 8.1 ± 3.6 mSv.

CT analyses

After CT data acquisition, the data sets were copied to the 3-mensio workstation (3-mensio Valves, version 7.0, 3-mensio Medical Imaging BV) on the computer. All examinations were analyzed between 30-40% R-R intervals on the 3-mensio workstation (Fig. 1c). A curved axis was generated across the valve from the ascending aorta into the left ventricular outflow trace. The cross-sectional annular plane was obtained by determining the lowermost point of the valves. The annulus border was traced outside calcifications. The presence of a bicuspid aortic valve was confirmed with visualization of two semilunar cusps in both systole and diastole [5, 11]. We used the TAVR-directed classification of the bicuspid aortic valve morphology, which is based on heterogeneous leaflet morphologies and leaflet orientation [9].

Once the plots and annular borderline had been drawn manually, the maximum and minimum dimension, area and perimeter of the annulus were obtained. The perimeter was calculated as the length of the borderline and the area by direct planimetry. Calculations of the mean, perimeter-derived and area-derived diameters were performed as follows:

$$\text{Mean diameter (CTmean)} = (\text{maximum diameter} + \text{minimum diameter})/2$$

$$\text{Perimeter-derived diameter (CTperi)} = (\text{annulus perimeter})/p$$

$$\text{Area-derived diameter (CTarea)} = 2 \times \sqrt{\left(\frac{annulus \quad area}{\pi}\right)}$$

We used the eccentricity index (1 – minimum diameter/maximum diameter) to describe the ovality of the aortic annulus [12]. The shape of the aortic annulus was considered elliptical when the eccentricity index was > 0.1.

All patients were divided into three subgroups according to the predominant localization of aortic valve calcifications: subgroup 1, calcifications mainly of the aortic annulus; subgroup 2, calcifications mainly of the aortic cusps; subgroup 3, calcifications of both the annulus and cusps.

Intraoperative analyses

Intraoperative measurements of the aortic annulus were obtained by an experienced cardiovascular surgeon after aortic semilunar cusp resection and annulus decalcification. The standard metric sizer (size 19 to 30 mm, unit 1 mm; Aesculap) was used for sizing. Complete elastic fit of the possible biggest dilatator was defined as optimal. All measurements were repeated twice with the final measurements representing the mean of both measurements.

The 3DTEE and CT measurements of the aortic annulus served as the basis for the theoretical surgical valve size selection according to the following recommendations: a 19-mm valve for annulus diameters between 19.0 mm and 20.9 mm; a 21-mm valve for annulus diameters between 21.0 mm and 22.9 mm; a 23-mm valve for annulus diameters between 23.0 mm and 24.9 mm; a 25-mm valve for annulus diameters between 25.0 mm and 26.9 mm; and a 27 mm valve for annulus diameters between 27.0 mm and 28.9 mm. We compared the 3DTEE-recommended, CTmean-recommended, CTperi-recommended and the CTarea-recommended valve sizes with the actual valve size implanted. The SAPIEN 3 (Edwards Lifesciences) TAVR valve was theoretically selected according to 3DTEE, CTmean, CTperi, CTarea and intraoperative measurements, respectively. Patients were stratified according to the suggested surgical valve size by CTperi relative to the implanted surgical valve size: group large, larger surgical valve size by CTperi than the implanted surgical valve size; group same, same surgical valve size by CTperi as the implanted surgical valve size; group small, smaller surgical valve size by CTperi than the implanted surgical valve size.

Statistical analysis

Quantitative variables were expressed as mean ± SD and qualitative variables as frequencies. The interaction between body surface area (BSA) and aortic valve size was evaluated using the indexed formula: indexed diameter = diameter (mm) divided by body surface area (m^2). The different diameter measurements in the same patient were compared using Student's *t*-test for paired data. Categorical variables were summarized as frequencies (%) and compared using the Pearson χ^2 test or Fisher exact test where applicable. Linear regression analysis was used to assess the relationship between variables, and the correlation coefficient was calculated. Measurements were compared using Bland-Altman plots. Inter-observer agreement was evaluated by calculating intra-class correlation coefficients. The Cohen κ statistic was used to assess prosthesis size agreement among 3DTEE, CT and intraoperative related selections. All *p* values reported are two-sided, and *p* values < 0.05 were considered significant. Data analysis was conducted with SPSS version 20.0 (SPSS Inc.). To present Fig. 1 with satisfactory imaging quality, we thickened the lines and enhanced the colors using image processing (Photoshop 13.0, Adobe Systems).

Results

Of the 126 subjects enrolled, 22 were excluded for an unavailable prosthesis size ($n = 4$), poor CT image quality ($n = 11$) or an inadequate echocardiographic window ($n = 7$). Finally, 104 patients with BAV (mean age, 69.1 ± 6.2 years; 55.7% male) constituted the study population, and the STS score was 6.8 ± 3.2. The mean body mass index and body surface area were 23.2 ± 2.5 kg/m^2 and 1.7 ± 0.1 m^2, respectively. Notably, the eccentricity index of 0.21±0.07 indicated a pronounced oval shape of the annulus in BAVs.

The mean diameters and correlation coefficients are shown in Tables 1 and 2. Significant differences in the mean values and those indexed to BSA were both observed in all five calculations, while the area-derived and indexed area-derived diameters were only slightly higher than those obtained by intraoperative measurements (25.6 ± 2.1 mm vs. 25.3 ± 2.0 mm, $p < 0.001$; 15.5 ± 0.6 mm/m^2 vs. 15.3 ± 0.6 mm/m^2, $p < 0.001$). Good correlation was found between diameters measured by 3DTEE and those measured by intraoperative sizing ($r = 0.901$, $p < 0.001$), with mild underestimation by 3DTEE.

Table 1 2DTTE, 3DTEE and CT measurements of aortic annulus in comparison with intraoperative direct sizing

	OP	2D-TTE	3D-TEE	CTmean	CTarea	CTperi
Annulus diameter (mm)	25.3 ± 2.0	24.5 ± 2.1	24.8 ± 2.0	25.9 ± 2.1	25.6 ± 2.1	26.2 ± 2.2
p value[a]	-	<0.001	<0.001	<0.001	<0.001	<0.001
Correlation	-	0.855	0.901	0.905	0.932	0.913
p value[b]	-	<0.001	<0.001	<0.001	<0.001	<0.001
Mean difference (mm)	-	0.80	0.53	-0.86	-0.30	-0.67
Limits of agreement (mm)	-	-0.74 to 2.35	-0.72 to 1.78	-2.17 to 0.45	-1.36 to 0.75	-1.91 to 0.58
ICC	-	0.81	0.85	0.88	0.90	0.89
95% CI	-	0.63 to 0.90	0.67 to 0.92	0.76 to 0.94	0.81 to 0.95	0.79 to 0.95

ICC = intra-class correlation coefficient; CTmax = maximum annulus diameter by CT; CTmin = minimum annulus diameter by CT; CTmean = the mean of maximum and minimum annulus diameter by CT; CTperi = perimeter-derived annulus diameter by CT; CTarea = area-derived annulus diameter by CT; *p* value[a] = *p* value for differences of mean; *p* value[b] = *p* value for correlation

Values are expressed as mean ± SD or mean with 95% confidence intervals

Table 2 Indexed 2DTTE, 3DTEE and CT measurements of aortic annulus in comparison with indexed intraoperative direct sizing

	Indexed-OP	Indexed-2DTTE	Indexed-3DTEE	Indexed-CTmean	Indexed-CTarea	Indexed-CTperi
Indexed annulus diameter (mm/m^2)	15.3 ± 0.6	14.8 ± 0.7	15.0 ± 0.7	15.7 ± 0.7	15.5 ± 0.6	15.8 ± 0.7
p value[c]	-	<0.001	<0.001	<0.001	<0.001	<0.001
Correlation	-	0.569	0.691	0.703	0.724	0.608
p value[d]	-	<0.001	<0.001	<0.001	<0.001	<0.001
Mean difference (mm/m^2)	-	0.48	0.32	-0.51	-0.18	-0.41
Limits of agreement (mm/m^2)	-	-0.44 to 1.41	-0.44 to 1.08	-1.34 to 0.32	-0.83 to 0.47	-1.15 to 0.33

p value[c] = *p* value for differences of mean; *p* value[d] = *p* value for correlation. Abbreviations as in Table 1

Indexed = diameter divided by body surface area (m^2)

Although all five methods correlated well with the surgical measurements, CTarea showed the best correlation ($r = 0.932$, $p < 0.001$). In particular, the perimeter-derived diameter was markedly larger than that assessed in surgery by approximately one millimetre (26.2±2.2 mm vs 25.3±2.0 mm, $p < 0.001$).

Moreover, the correlations of indexed intraoperative sizing with indexed-CTperi ($r = 0.608$, $p < 0.001$) were weaker than those with indexed-CTarea, indexed-CTman and indexed-3DTEE ($r = 0.724$, $p < 0.001$; $r = 0.703$, $p < 0.001$; $r = 0.691$, $p < 0.001$, respectively). CTarea and CTperi were found to be more reproducible than other measurements (ICC 0.90, 95% CI 0.81 to 0.95; ICC 0.89, 95% CI 0.79 to 0.95).

Figures 2 and 3 showed the related scatter plots with regression together with the results of Bland-Altman analysis for annulus diameters and indexed annulus diameters. The diameters measured by 3DTEE were systematically smaller than those by intraoperative sizing (mean difference, 0.53

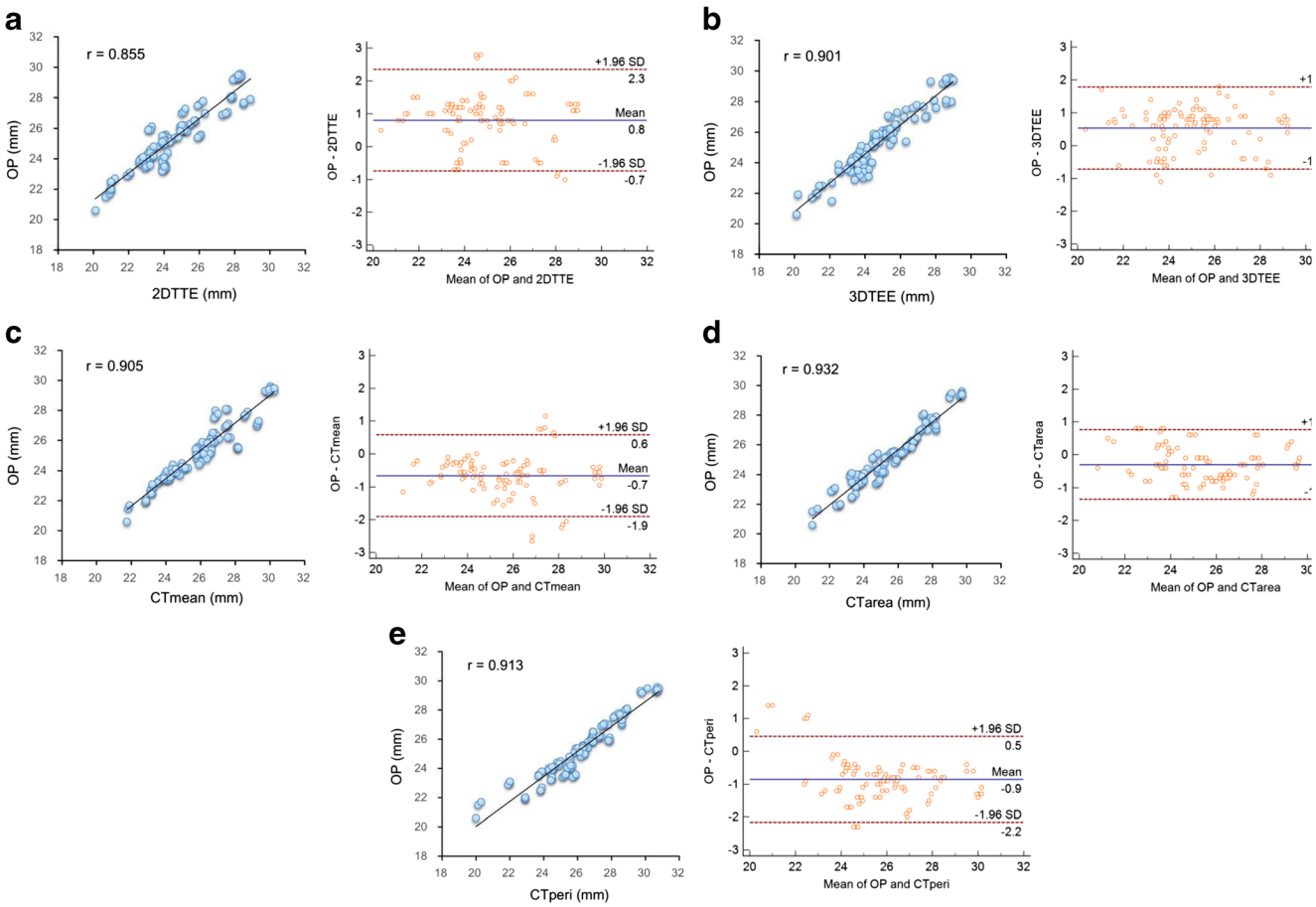

Fig. 2 Line regression (left panels) and Bland-Altman analysis (right panels) comparing annulus sizing by 2DTTE, 3DTEE, CT (CTmean, CTarea, CTperi) and intraoperative measurement. For the Bland-Altman analysis, the horizontal solid line expresses the mean value of difference, whereas the plot lines express the limits of agreement defined as mean ± 1.96*SD

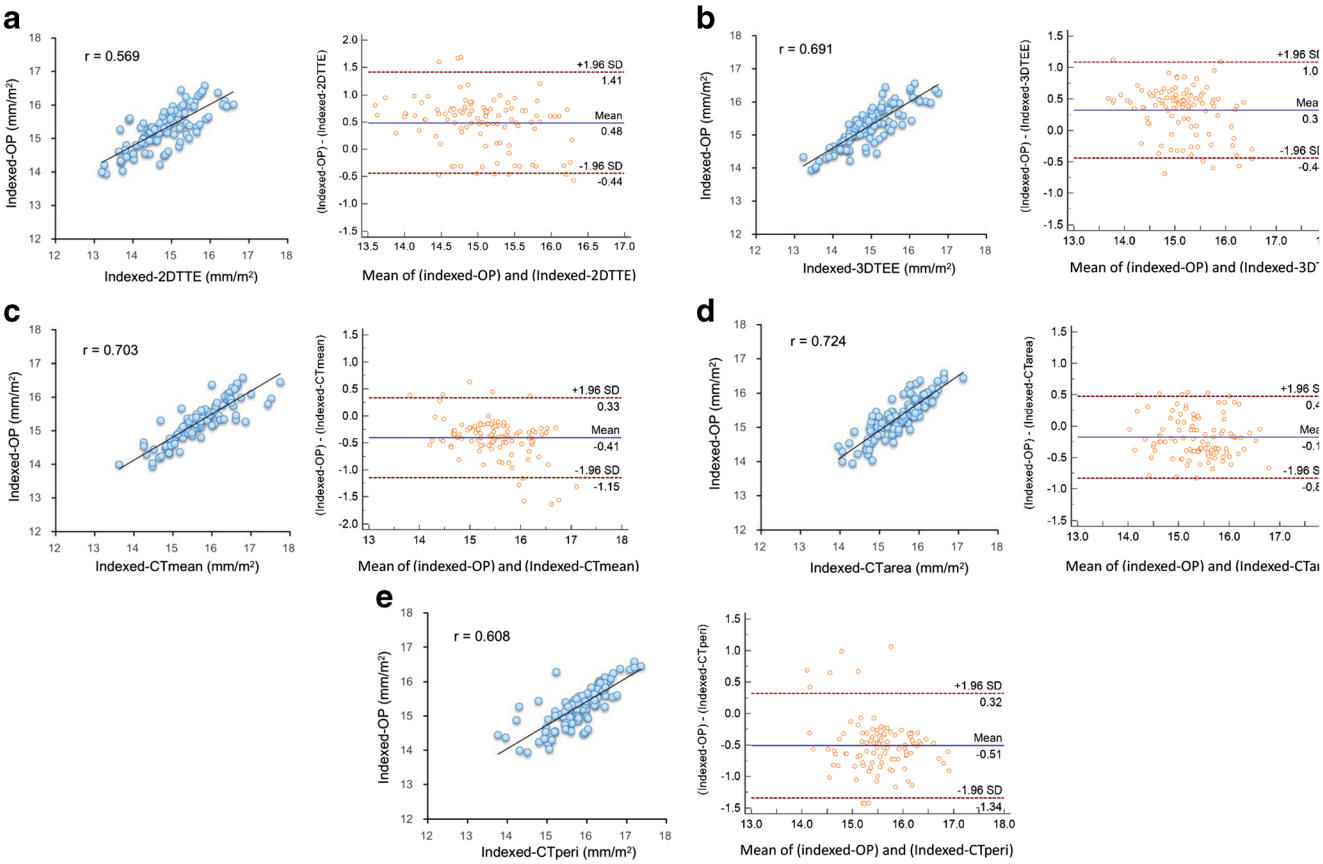

Fig. 3 Line regression (left panels) and Bland-Altman analysis (right panels) comparing indexed annulus sizing by 2DTTE, 3DTEE, CT (CTmean, CTarea, CTperi) and intraoperative measurement. For the Bland-Altman analysis, the horizontal solid line expresses the mean value of difference, whereas the plot lines express the limits of agreement defined as mean ± 1.96*SD

mm; limits of agreement, -0.72 mm to 1.78 mm). CTarea showed sufficient agreement with the intraoperative measurements, with the best limits of agreement observed in the Bland-Altman analysis (Table 1 and Fig. 2). As shown in Fig. 3, the agreement with intraoperative sizing was better for indexed-CTmean than indexed-CTperi; these measurements featured smaller mean differences with narrower variation (mean difference, -0.18 mm/m^2; limits of agreement, -0.83 mm/m^2 to 0.47 mm/m^2; mean difference, -0.41 mm/m^2; limits of agreement, -1.15 mm/m^2 to 0.33 mm/m^2, respectively).

No significant differences in baseline characteristics were observed among the three subgroups (Supplementary Table A). Diameters of all three subgroups measured by CT were slightly but significantly larger than those measured intraoperatively (Table 3). Good correlations were observed between the two measurements regardless of the predominant site of aortic valve calcification (r = 0.860-0.953). The agreements between measurements were greater for CTarea than for CTperi and CTmean. Reliability assessment of the CT measurements showed superior reproducibility than that of 3DTEE and 2DTTE measurements.

The measurements performed by 3DTEE were statistically lower than those obtained intraoperatively in all three subgroups. The correlation between the two methods was good for patients with predominantly calcified cusps ($r = 0.924$, $p < 0.001$), but it was slightly reduced for patients with calcifications mainly of the annulus ($r = 0.825$, $p < 0.001$) and patients with calcifications of both annulus and cusps ($r = 0.853$, $p < 0.001$). The limits of agreement for patients with a predominantly calcified annulus were the broadest (limits, -0.7 mm to 2.1 mm) among the three subgroups, with the lowest intraobserver reliability (ICC 0.80, 95% CI 0.49 to 0.93).

The theoretical selections of the surgical valve and Sapien 3 TAVR valve according to the measurements of 3DTEE, CTmean, CTarea and CTperi are illustrated in Table 4. CTarea-based selections of the surgical prosthesis agreed best ($\kappa = 0.791$, $p < 0.001$) with the actual surgical valve implanted in 84.6% (n = 88) of BAVs, with over- or undersizing in 12.5% and 2.9% of patients, respectively. In 74.0% (n = 77) of cases, the theoretical TAVR prosthesis size was concordant with the CTarea and intraoperative data. However, agreements between CTperi-based selections and surgical valve or TAVR valve were the lowest ($\kappa = 0.598$, $p < 0.001$; $\kappa = 0.425$, $p <$

Table 3 2DTTE, 3DTEE and CT measurements of aortic annulus compared with intraoperative direct sizing in three subgroups according to the predominant localization of aortic valve calcification

	OP	2D-TTE	3D-TEE	CTmean	CTarea	CTperi
Calcification mainly of aortic annulus						
Annulus diameter (mm)	25.3 ± 1.7	24.0 ± 1.7	24.7 ± 1.8	25.9 ± 1.7	25.6 ± 1.8	26.0 ± 1.9
p value[a1]	-	<0.001	<0.001	<0.001	<0.001	<0.001
Correlation	-	0.877	0.825	0.879	0.924	0.888
p value[b1]	-	<0.001	<0.001	<0.001	<0.001	<0.001
Mean difference (mm)	-	1.24	0.70	-0.67	-0.36	-0.78
Limits of agreement (mm)	-	0.11 to 2.37	-0.70 to 2.10	-1.81 to 0.47	-1.33 to 0.61	-2.00 to 0.44
ICC	-	0.75	0.80	0.88	0.90	0.86
95% CI	-	0.41 to 0.91	0.49 to 0.93	0.67 to 0.96	0.72 to 0.96	0.64 to 0.95
Calcification mainly of aortic cusps						
Annulus diameter (mm)	25.5 ± 2.3	24.8 ± 2.3	25.0 ± 2.7	26.0 ± 2.3	25.6 ± 2.3	26.3 ± 2.4
p value[a2]	-	<0.001	<0.001	<0.001	<0.001	<0.001
Correlation	-	0.861	0.924	0.923	0.953	0.929
p value[b2]	-	<0.001	<0.001	<0.001	<0.001	<0.001
Mean difference (mm)	-	0.63	0.46	-0.60	-0.17	-0.87
Limits of agreement (mm)	-	-1.07 to 2.32	- 0.76 to 1.69	-1.84 to 0.65	-1.14 to 0.80	-2.13 to 0.38
ICC	-	0.82	0.88	0.89	0.91	0.91
95% CI	-	0.71 to 0.89	0.80 to 0.93	0.82 to 0.93	0.85 to 0.95	0.85 to 0.94
Calcifications of both the annulus and cusps						
Annulus diameter (mm)	25.5 ± 2.3	24.2 ± 1.7	24.5 ± 1.6	25.8 ± 1.8	25.6 ± 1.8	25.9 ± 2.1
p value[a3]	-	<0.001	<0.001	<0.001	<0.001	<0.001
Correlation	-	0.855	0.853	0.860	0.903	0.895
p value[b3]	-	<0.001	<0.001	<0.001	<0.001	<0.001
Mean difference (mm)	-	0.90	0.58	-0.78	-0.50	-0.86
Limits of agreement (mm)	-	-0.36 to 2.16	-0.64 to 1.79	-2.07 to 0.50	-1.63 to 0.63	-2.34 to 0.61
ICC	-	0.79	0.81	0.87	0.89	0.87
95% CI	-	0.62 to 0.89	0.64 to 0.90	0.75 to 0.93	0.80 to 0.95	0.76 to 0.94

p value[a1], *p* value[a2], *p* value[a3]: *p* value for differences of mean; *p* value[b1], *p* value[b2], *p* value[b3]: *p* value for correlation

Abbreviations as in Table 1. Values are mean ± SD or mean with 95% confidence intervals

0.001, respectively) in comparison to those between intraoperative sizing and the other three measurements. The size of the selected TAVR prosthesis would have been larger in 36.5% (n = 38) of BAVs if the perimeter-derived diameter had been used instead of intraoperative sizing. However, the prevalence of a larger valve size recommendation was only

Table 4 Impact of measurements on choice of surgical and SAPIEN 3 prosthesis size

	3D-TEE	κ Cohen	CTmean	κ Cohen	CTperi	κ Cohen	CTarea	κ Cohen
Surgical valve								
More than 1 valve-size overestimation	10 (9.6%)	0.600	21 (20.2%)	0.642	28 (26.9%)	0.589	13 (12.5%)	0.791
Proper valve-size choice	67 (64.4%)	$p < 0.001$	77 (74.0%)	$p < 0.001$	72 (69.2%)	$p < 0.001$	88 (84.6%)	$p < 0.001$
More than 1 valve-size underestimation	27 (26.0%)		6 (5.8%)		4 (3.8%)		3 (2.9%)	
SAPIEN 3 valve								
More than 1 valve-size overestimation	6 (5.8%)	0.507	30 (28.8%)	0.531	38 (36.5%)	0.425	22 (21.2%)	0.585
Proper valve-size choice	75 (72.1%)	$p < 0.001$	73 (70.2%)	$p < 0.001$	66 (63.5%)	$p < 0.001$	77 (74.0%)	$p < 0.001$
More than 1 valve-size underestimation	23 (22.1%)		1 (1.0%)		0 (0.0%)		5 (4.8%)	

Abbreviations as in Table 1

21.2% ($n = 22$) using area-derived sizing. Of the 38 cases with TAVR prosthesis oversizing by CTperi, 17 (44.7%) would have been correctly identified by CTarea.

Baseline and procedural characteristics and postoperative outcomes are presented in Table 5. All the preoperative data, the BAV morphology in particular, were comparable among the three groups. There was only one patient in Group-large who died within 30 days after the surgery, and there were no significant differences in procedural or 30-day outcomes.

Table 5 Comparison of basic characteristics and outcomes among three groups (Group same, Group large and Group small)

	Group same ($n = 72$)	Group large ($n = 28$)	Group small	p^e ($n = 4$)	p^f
Clinical characteristics					
Age (years)	69.3 ± 6.2	68.1 ± 6.4	73.3 ± 2.8	0.384	0.165
BMI (kg/m^2)	23.6 ± 2.7	23.3 ± 1.8	22.9 ± 2.2	0.485	0.671
BSA (m^2)	1.7 ± 0.1	1.7 ± 0.1	1.6 ± 0.1	0.684	0.761
STS PROM score	6.9 ± 3.2	6.8 ± 3.4	4.0 ± 1.1	0.573	0.095
Diabetes mellitus (%)	15 (20.8)	4 (14.3)	0 (0)	0.576	0.579
COPD (%)	13 (18.1)	4 (14.3)	1 (25.0)	0.773	0.565
NYHA IV (%)	4 (5.6)	3 (10.7)	0 (0)	0.396	1
BAV morphology				0.557	0.879
Tricommissural BAV	16 (22.2)	7 (25.0)	1 (25.0)		
Bicommissural BAV with raphe	36 (50.0)	15 (53.6)	2 (50.0)		
Bicommissural BAV without raphe	20 (27.8)	6 (21.4)	1 (25.0)		
Preoperative echocardiographic characteristics					
Peak velocity (m/s)	5.0 ± 0.7	4.8 ± 0.6	5.2 ± 1.1	0.151	0.118
Mean gradient (mmHg)	60.9 ± 18.2	59.2 ± 22.5	65.8 ± 35.2	0.145	0.122
Peak gradient (mmHg)	102.2 ± 27.8	94.8 ± 24.1	106 ± 25.5	0.139	0.181
LVEF (%)	55.4 ± 11.8	55.2 ± 13.4	61.7 ± 9.9	0.189	0.721
Predominant site of calcifications				0.698	0.755
Aortic annulus (%)	9 (12.5)	4 (14.3)	2 (50.0)		
Aortic cusps (%)	42 (58.3)	14 (50.0)	0 (0.0)		
Both the annulus and cusps (%)	21 (29.2)	10 (35.7)	2 (50.0)		
Procedural outcomes					
Mortality (%)	0 (0)	0 (0)	0 (0)	-	-
Stroke (%)	1 (1.4)	0 (0)	0 (0)	1	1
Reoperation for bleeding (%)	1 (1.4)	0 (0)	1 (25.0)	1	0.103
Multisystem failure (%)	1 (1.4)	0 (0)	0 (0)	1	1
30-day outcomes					
Mortality (%)	0 (0)	1 (3.6)	0 (0)	0.280	-
AKI ≥ stage 3 (%)	1 (1.4)	1 (3.6)	1 (25.0)	0.484	0.103
Cerebrovascular event (%)	0 (0)	1 (3.6)	0 (0)	0.280	-
PVL ≥ moderate (%)	0 (0)	0 (0)	0 (0)	-	-
Postoperative echocardiographic characteristics					
Peak velocity (m/s)	2.2 ± 0.5	2.2 ± 0.5	2.2 ± 0.5	0.573	0.182
Mean gradient (mmHg)	10.2 ± 5.1	10.5 ± 4.8	10.3 ± 3.2	0.625	0.575
Peak gradient (mmHg)	19.6 ± 8.8	21.3 ± 8.9	19.3 ± 4.3	0.288	0.396
LVEF (%)	65.1 ± 5.8	62.2 ± 8.0	63.3 ± 1.5	0.107	0.069

AKI = acute kidney injury; BMI = body mass index; BSA = body surface area; COPD = chronic obstructive pulmonary disease; LVEF = left ventricular ejection fraction; PVL = paravalvular leak; STS PROM = Society of Thoracic Surgeons Predicted Risk of Mortality; NYHA = New York Heart Association; p^e = p value for Group same vs. Group large; p^f = p value for Group same vs. Group small

Values are expressed as mean ± SD or n (%)

Discussion

The main findings of our study are as follows: (1) In BAV patients referred for TAVR, area-derived assessment by CT as well as decisions for surgical or TAVR prosthesis size showed the best agreement with intraoperative sizing. (2) Perimeter-derived sizing based on CT was prone to overestimate the annulus size. (3) 3DTEE slightly underestimated the aortic annulus dimensions compared with intraoperative sizing, particularly in patients with calcified annulus.

Due to the media degeneration, altered hemodynamics and more oval aortic annulus of BAVs [13, 14], post-implantation reformation, which is a strong determinant of impending complications, is more likely in BAVs than in TAVs. Therefore, precise preprocedural bicuspid annulus sizing is critical to guarantee successful intraprocedural valve positioning and to avoid pitfalls. Moreover, with increasing worldwide numbers of implantations for BAVs and considerably high proportions of BAVs among Chinese TAVR patients (up to 67%) [15], optimal and standardized sizing is required.

Inevitable underestimation of 2DTTE or 2DTEE, caused by the off-axis measurements, has already been shown [16]. Our data additionally showed the significantly poor accuracy of 2DTTE-based sizing for elliptical annulus of BAVs. Three-dimensional visualization of the complex crown-like aortic root by CT or 3DTEE has been considered the reference standard for annulus sizing [17]. For CT in particular, several previous studies have shown systematic differences between systolic and diastolic measurements for the cross-sectional maximum diameter, minimum diameter, perimeter and area [18]. The systolic phase, typically a 30-40% R-R interval based on the image quality, is considered the reference phase for analyses to avoid under-sizing of the prosthesis [5, 19]. Although several studies have described the comparisons of non-invasive imaging methods with direct intraoperative measurement, there is no consensus regarding the optimal calculation method (e.g., the mean, area-derived or perimeter-derived diameters) for a prosthesis chosen by CT. In addition, information on the most precise approach to BAV sizing remains limited.

Kempfert and colleagues assessed 26 patients and pointed out that the best agreement with intraoperative sizing was given by the area-derived diameter obtained by CT [20]. Notably, due to the conformational pulsatile changes of the aortic annulus during the cardiac cycle, measurements at diastole in Kempfert's study could result in underestimation of that value [5]. Wang et al compared the area-derived diameter with the direct intraoperative dimension and performed analyses of BAVs versus TAVs [21]. The data of the former comparison showed consistence with Kempfert's study, whereas the findings indicating no significant difference in eccentricity between the two valve phenotypes conflicted with reports in previous large TAVR registries [22]. Although overestimation by CT was noticed in 46.3% of cases in the study by Wang et al, the inhomogeneous CT imaging and the fact that few of the CT scans were ECG-gated could be the source of the limitation. The study by Kim and co-workers first involved 52 TAVR-like patients and demonstrated that area-derived sizing performed better than perimeter-derived sizing; however, the eccentricity of the annulus and morphology of the aortic valve were not reported [23]. Notably, the cyclic variability of a subset of patients is relatively large and may lead to different choices of prosthesis sizes, indicating the necessity of exploring the optimal measurement for deformation-prone BAVs.

As the first study comparing the three imaging techniques (2DTTE, 3DTEE and CT) with intraoperative sizing for BAV patients assigned for TAVR, we recommend the area-derived diameter by CT as the most appropriate parameter for accurate sizing. The most appropriate theoretical prosthesis choice based on the area-derived diameter is clearly demonstrated in Table 4. Based on the findings listed in Tables 1, 2 and Fig. 2, 3DTEE sizing showed good agreement following area-derived measurement, but it was not as reproducible as the perimeter- and area-derived approaches. The inter-observer variance of point placement on the BAV annulus may be attributed to the observed smaller intraclass correlation coefficient for CTmean, but this inaccuracy is offset when evaluating the area or perimeter.

One factor that may influence the accuracy of aortic annulus sizing is aortic valve calcifications. Previous studies have investigated the influence of aortic valve calcifications on the agreement between echocardiography and CT for aortic annulus sizing, but in the absence of a truly validated gold standard [24, 25]. With direct intraoperative sizing as the gold standard, we divided all patients with BAV into three subgroups according to the predominant localization of aortic valve calcifications. Close correlations were found between intraoperative measurements and those by CT in all three subgroups. Slightly reduced agreement between 3DTEE and intraoperative sizing was noted in patients with calcifications mainly of the aortic annulus compared with that in the other subgroups, which may be due to the lower spatial resolution associated with 3DTEE volumetric imaging, impeding clear delineation of the aortic annulus. Calcifications at the aortic annulus, which cause partial acoustic shadowing of the aortic annulus, hamper the accuracy of the tracing of the aortic annulus by 3DTEE. In contrast, CT provides superior blood/tissue contrast, even in the presence of calcium. With the strongest calcification-independent correlation and the highest level of reproducibility, CTarea should therefore be considered the most reliable measurement of aortic annulus sizing.

Notably, our study demonstrated that perimeter-derived dimensions could lead to an overestimation of the annulus size, which suggested the need for a larger prosthesis, and were inferior to area-derived measurements for valve selection. In our cohort, 26.9% of the patients would have

received a larger surgical valve according to CTperi and more than one TAVR valve size in 36.5% of BAVs. Our data are partly consistent with the study by George et al in which CTperi-based sizing led to valve size overestimation in 41% of patients [26]. One possible reason lies in the geometric principle of post-implantation deformation from an ellipse to circle or approximate circle. The area-derived perimeter is smaller than the other two approaches in the same oval annulus. With increasing eccentricity of the annulus, the difference between CTarea and CTmean increases, as does that between CTarea and CTperi. Theoretically, the TAVR valve will expand to the size of the native aortic annulus area. Therefore, the excessive overestimation produced by CTperi- or CTmean-based prosthesis selection may happen and would be more serious in an extremely elliptical-shaped annulus. Additionally, dramatically decreased elasticity caused by the degenerated media of BAVs would weaken the tolerance of the aortic wall against radio-force of unduly oversized implantations. Although no short-term clinical or postoperative echocardiographic data were apparent from under- or oversizing of surgical valves selected by CTperi in our study, fatal complications and poor prognoses could occur if post-dilatation of TAVR was performed in these cases with overestimation. Therefore, the conservative area-derived perimeter would be preferable for valve size selection for BAVs, particularly among BAV patients with borderline annulus and thickened or calcified valves.

All these data show that the area-derived diameter provides more accurate information for BAVs than the perimeter-derived diameter with superior discrimination of the aorto-iliofemoral arterial pathway. However, the trend of overestimation for perimeter-derived BAV sizing reflects a bias due to its geometric nature, and in some cases, it may result in a higher risk of oversizing-related complications. Furthermore, the multifactorial approaches for pre-TAVR measurement, including balloon aortic valvuloplasty, magnetic resonance imaging (MRI) [27] and three-dimensional printing [28], should also be highlighted. With the recognition of super-annulus assessment complementary to valve sizing [29], more standardized and detailed sizing procedures tailored to BAV patients for TAVR would contribute to a better informed valve choice.

Limitations

The limitations of this study include those inherent to a single-institution study with retrospective analysis of observational data. Although we elucidated solid statistical significance between different sizing approaches in our sample size of 104 patients, further studies may be needed to evaluate MRI, three-dimensional printing and other modalities in larger cohorts to provide greater clinical evidence. Another limitation was the incapability to verify the potential impact on long-term clinical outcomes in our study design. Lastly, there could be potential bias owing to pre-intraoperative sizing decalcification, while exclusion of intra-annular calcifications from CT measurements would reduce this error.

Conclusion

Area-derived sizing by CT for annulus measurement as well as surgical or TAVR prosthesis selection for pre-TAVR patients with BAV showed the best agreement with intraoperative sizing. CTperi was prone to overestimation and CTmean was not as reproducible as CTarea. Close and mostly calcification-independent correlations were found between CT and intraoperative sizing. 3DTEE could represent a valid alternative for BAVs unsuitable for CT. However, it should be used with caution among patients experiencing annulus calcification as partial acoustic shadowing could lead to image inaccuracy. For BAVs with a greater likelihood of reshaping and deformation, especially those with borderline annulus, the predominance of CTarea-based annulus sizing should be emphasized and included into the BAV-specific annulus sizing recommendation. More standardized and detailed sizing procedures tailored to BAVs should be formulated.

Acknowledgements The authors thank the staff members of the imaging department for their invaluable contribution.

Funding This study was supported by grants from the Pecking Union Medical College Student Innovation Fund (project no. 2016-1002-01-05, Beijing, China) to YW.

Compliance with ethical standards

Guarantor The scientific guarantor of this publication is Dr. Yongjian Wu.

Conflict of interest The authors of this manuscript declare no relationships with any companies, whose products or services may be related to the subject matter of the article.

Statistics and biometry One of the authors has significant statistical expertise.

Informed consent Written informed consent was obtained from all subjects (patients) in this study.

Ethical approval Institutional Review Board approval was obtained.

Methodology
- retrospective
- randomized controlled trial
- performed at one institution

References

1. Mack MJ, Leon MB, Smith CR et al (2015) 5-year outcomes of transcatheter aortic valve replacement or surgical aortic valve replacement for high surgical risk patients with aortic stenosis (PARTNER 1): a randomised controlled trial. Lancet 385:2477–2484
2. Perlman GY, Blanke P, Dvir D et al (2016) Bicuspid aortic valve stenosis: favorable early outcomes with a next-generation transcatheter heart valve in a multicenter study. JACC Cardiovasc Interv 9:817–824
3. Pontone G, Andreini D, Bartorelli AL et al (2012) Aortic annulus area assessment by multidetector computed tomography for predicting paravalvular regurgitation in patients undergoing balloon-expandable transcatheter aortic valve implantation: a comparison with transthoracic and transesophageal echocardiography. Am Heart J 164:576–584
4. Nishimura RA, Otto CM, Bonow RO et al (2014) 2014 AHA/ACC guideline for the management of patients with valvular heart disease: a report of the American College of Cardiology/American Heart Association Task Force on Practice Guidelines. J Thorac Cardiovasc Surg 148:e1–e132
5. Otto CM, Kumbhani DJ, Alexander KP et al (2017) 2017 ACC Expert Consensus Decision Pathway for Transcatheter Aortic Valve Replacement in the Management of Adults with Aortic Stenosis: A Report of the American College of Cardiology Task Force on Clinical Expert Consensus Documents. J Am Coll Cardiol 69:1313–1346
6. Wijesinghe N, Ye J, Rodés-Cabau J et al (2010) Transcatheter aortic valve implantation in patients with bicuspid aortic valve stenosis. JACC Cardiovasc Interv 3:1122–1125
7. Hayashida K, Bouvier E, Lefèvre T et al (2013) Transcatheter aortic valve implantation for patients with severe bicuspid aortic valve stenosis. Circ Cardiovasc Interv 6:284–291
8. Stolzmann P, Leschka S, Scheffel H et al (2008) Dual-source CT in step-and-shoot mode: noninvasive coronary angiography with low radiation dose. Radiology 249:71–80
9. Jilaihawi H, Chen M, Webb J et al (2016) A bicuspid aortic valve imaging classification for the TAVR Era. JACC Cardiovasc Imaging 9:1145–1158
10. Kerl JM, Ravenel JG, Nguyen SA et al (2008) Right heart: split-bolus injection of diluted contrast medium for visualization at coronary CT angiography. Radiology 247:356–364
11. Shin HJ, Shin JK, Chee HK et al (2015) Characteristics of aortic valve dysfunction and ascending aorta dimensions according to bicuspid aortic valve morphology. Eur Radiol 25:2103–2114
12. Vaquerizo B, Spaziano M, Alali J et al (2016) Three-dimensional echocardiography vs. computed tomography for transcatheter aortic valve replacement sizing. Eur Heart J Cardiovasc Imaging 17:15–23
13. Schnell S, Smith DA, Barker AJ et al (2016) Altered aortic shape in bicuspid aortic valve relatives influences blood flow patterns. Eur Heart J Cardiovasc Imaging 17:1239–1247
14. Pham T, Martin C, Elefteriades J et al (2013) Biomechanical characterization of ascending aortic aneurysm with concomitant bicuspid aortic valve and bovine aortic arch. Acta Biomater 9:7927–7936
15. Zhao ZG, Jilaihawi H, Feng Y et al (2015) Transcatheter aortic valve implantation in bicuspid anatomy. Nat Rev Cardiol 12:123–128
16. Yano M, Nakamura K, Nagahama H et al (2012) Aortic annulus diameter measurement: what is the best modality? Ann Thorac Cardiovasc Surg 18:115–120
17. Tamborini G, Fusini L, Muratori M et al (2014) Feasibility and accuracy of three-dimensional transthoracic echocardiography vs. multidetector computed tomography in the evaluation of aortic valve annulus in patient candidates to transcatheter aortic valve implantation. Eur Heart J Cardiovasc Imaging 15:1316–1323
18. Jurencak T, Turek J, Kietselaer BL et al (2015) MDCT evaluation of aortic root and aortic valve prior to TAVI. What is the optimal imaging time point in the cardiac cycle? Eur Radiol 25:1975–1983
19. Murphy DT, Blanke P, Alaamri S et al (2016) Dynamism of the aortic annulus: Effect of diastolic versus systolic CT annular measurements on device selection in transcatheter aortic valve replacement (TAVR). J Cardiovasc Comput Tomogr 10:37–43
20. Kempfert J, Van Linden A, Lehmkuhl L et al (2012) Aortic annulus sizing: echocardiographic versus computed tomography derived measurements in comparison with direct surgical sizing. Eur J Cardiothorac Surg 42:627–633
21. Wang H, Hanna JM, Ganapathi A et al (2015) Comparison of aortic annulus size by transesophageal echocardiography and computed tomography angiography with direct surgical measurement. Am J Cardiol 115:1568–1573
22. Salaun E, Zenses AS, Evin M et al (2016) Effect of oversizing and elliptical shape of aortic annulus on transcatheter valve hemodynamics: an in vitro study. Int J Cardiol 208:28–35
23. Kim WK, Meyer A, Mollmann H et al (2016) Cyclic changes in area- and perimeter-derived effective dimensions of the aortic annulus measured with multislice computed tomography and comparison with metric intraoperative sizing. Clin Res Cardiol 105:622–629
24. Rixe J, Schuhbaeck A, Liebetrau C et al (2012) Multi-detector computed tomography is equivalent to trans-oesophageal echocardiography for the assessment of the aortic annulus before transcatheter aortic valve implantation. Eur Radiol 22:2662–2669
25. Podlesnikar T, Prihadi EA, van Rosendael PJ et al (2018) Influence of the quantity of aortic valve calcium on the agreement between automated 3-dimensional transesophageal echocardiography and multidetector row computed tomography for aortic annulus sizing. Am J Cardiol 121:86-93
26. George I, Guglielmetti LC, Bettinger N et al (2017) Aortic valve annular sizing: intraoperative assessment versus preoperative multidetector computed tomography. Circ Cardiovasc Imaging 10(5). https://doi.org/10.1161/CIRCIMAGING.116.005968
27. Ruile P, Blanke P, Krauss T et al (2016) Pre-procedural assessment of aortic annulus dimensions for transcatheter aortic valve replacement: comparison of a non-contrast 3D MRA protocol with contrast-enhanced cardiac dual-source CT angiography. Eur Heart J Cardiovasc Imaging 17:458–466
28. Schmauss D, Schmitz C, Bigdeli AK et al (2012) Three-dimensional printing of models for preoperative planning and simulation of transcatheter valve replacement. Ann Thorac Surg 93:31–33
29. Patsalis PC, Al-Rashid F, Neumann T et al (2013) Preparatory balloon aortic valvuloplasty during transcatheter aortic valve implantation for improved valve sizing. JACC Cardiovasc Interv 6:965–971